gorder: Comprehensive tool for calculating lipid order parameters from molecular simulations

Ladislav Bartoš[a,b,*], Peter Pajtinka[a,b], Robert Vácha[a,b,c,*]

[a] *CEITEC – Central European Institute of Technology, Kamenice 753/5, 625 00 Brno, Czech Republic*
[b] *National Centre for Biomolecular Research, Faculty of Science, Masaryk University, Kamenice 753/5, 625 00 Brno, Czech Republic*
[c] *Department of Condensed Matter Physics, Faculty of Science, Masaryk University, Kotlářská 267/2, 611 37 Brno, Czech Republic*

Abstract

Lipid order parameters are an important metric for quantifying the molecular structure of biological membranes. They can be derived from both molecular simulations and experimental measurements, enabling robust comparisons between the two. Although methods for calculating lipid order parameters from molecular dynamics simulations of membrane systems at various resolutions are well established, a comprehensive and user-friendly package for these calculations is lacking, which has even led some researchers to use tools that are known to perform the calculations incorrectly. To address this, we have developed `gorder`, an analysis tool capable of calculating lipid order parameters in atomistic, united-atom, and coarse-grained systems, compatible with any force field, and applicable to both planar and curved membrane geometries. `gorder` is designed to be fast and versatile, providing a unified solution for lipid order calculations. The tool is freely available from `crates.io/crates/gorder` and `github.com/Ladme/gorder` under the MIT License.

Keywords: lipid order parameters, molecular dynamics, membranes, molecular dynamics analysis, Gromacs

*Corresponding author.
Email addresses: `ladmeb@gmail.com` (Ladislav Bartoš), `robert.vacha@muni.cz` (Robert Vácha)

Metadata

Nr.	Code metadata description	Metadata
C1	Current code version	v0.7.1
C2	Permanent link to code/repository used for this code version	`https://github.com/Ladme/gorder`
C3	Permanent link to Reproducible Capsule	–
C4	Legal Code License	MIT License
C5	Code versioning system used	git
C6	Software code languages, tools, and services used	Rust, C, Python
C7	Compilation requirements, operating environments & dependencies	required: rustc, cargo, gcc/clang/msvc; recommended: python, uv
C8	If available, link to developer documentation/manual	`https://ladme.github.io/gorder-manual/`
C9	Support email for questions	ladmeb@gmail.com

Table 1: Code metadata

1. Motivation and significance

Lipid order parameters quantify the degree of ordering in phospholipid membranes. In the field of molecular dynamics, they are widely used for assessing force field accuracy [1, 2, 3, 4, 5, 6, 7], studying membrane structures [8, 9, 10, 11, 12, 13, 14, 15], tracking phase transitions [16, 17], and various other applications [18, 19, 20]. The term "lipid order parameters" typically refers to one of two related but distinct metrics: S_{CH} and S_{CC} order parameters.

The S_{CH} (sometimes referred to as S_{CD}) order parameters are associated with bonds between heavy atoms (typically carbons) and hydrogens. The absolute values of S_{CH} order parameters can also be obtained experimentally using quadrupolar splitting from deuterium NMR experiments [21, 22] or dipolar splitting measured using carbon-13 NMR experiments [23, 24, 25], rendering this metric particularly useful.

For coarse-grained systems, where multiple heavy atoms and their bonded hydrogens are coalesced into a single bead, this metric is not applicable. Instead, the S_{CC} order parameters can be used, which relate to bonds between two consecutive beads of the lipid molecule [26]. While S_{CC} order parameters

are not directly quantitatively comparable to the experimentally measured S_{CH} order parameters, they represent the same physical properties.
In the following text, we will refer to S_{CH} order parameters calculated using explicit hydrogen positions as "atomistic order parameters," S_{CH} order parameters calculated using predicted hydrogen positions as "united-atom order parameters," and S_{CC} order parameters as "coarse-grained order parameters."
The calculation of atomistic, united-atom, and coarse-grained order parameters is relatively well established, with various tools available for computing them from molecular dynamics simulations, including those designed for the popular GROMACS simulation package [27].
In the GROMACS community, a widely used tool for calculating S_{CH} order parameters is `gmx order`, which is included in the GROMACS simulation package. `gmx order` computes *united-atom* order parameters, implicitly predicting hydrogen positions during the calculation, even if the hydrogens are explicitly available. However, it has been demonstrated that `gmx order` does not correctly calculate order parameters for unsaturated carbons [28]. These findings prompted the GROMACS developers to remove this option entirely from the tool, and `gmx order` is now explicitly marketed as a tool applicable exclusively for analyzing fully saturated united-atom lipid tails [29].
Despite this requirement, the tool is frequently employed in scenarios that contradict it. Since 2020 alone, we have identified at least 16 scientific publications where `gmx order` was applied to unsaturated carbons in atomistic systems [30, 31, 32, 33, 34, 35, 36, 37, 38, 39, 40, 41, 42, 43, 44, 45], 3 articles where it was used to calculate order parameters for unsaturated carbons in united-atom systems [46, 47, 48], and even 2 articles where it was used for coarse-grained systems [49, 50], despite the inherent contradiction of predicting hydrogen positions for coarse-grained lipids. Additionally, `gmx order` is very frequently employed to calculate order parameters for saturated carbons in *atomistic* systems (see, e.g., [51, 52, 53, 54, 55, 56, 57, 58, 59, 60]). While for these saturated carbons, the errors introduced by predicting hydrogen positions are typically small and often negligible, this usage of `gmx order` still goes against the recommendation.
There are some alternatives to `gmx order` that are generally better suited for calculating order parameters. For atomistic systems, one can use tools such as scripts provided by NMR Lipids [61], VMD's `calc_op.tcl` script [62], or the `order_params` tool included in the LOOS library [63, 64]. For united-atom systems, the `g_lomepro` package (available from github.com/vgapsys/g_lomepro) or the `buildH` tool [65] can be employed, both of which handle unsaturated carbons correctly. For coarse-grained systems, options include the `do-order` script (available from cgmartini.nl/docs/downloads/tools/other-tools.html)

provided by the developers of the Martini force field [66, 67], the `lipyphilic` library [68], or the `order` program [69], a tool previously developed by one of the authors of this article. Additionally, some researchers develop in-house tools tailored to their specific needs.

Despite the availability of these alternatives, the use of `gmx order` persists. This is largely due to its direct inclusion in the GROMACS simulation package, making it immediately accessible for many researchers. Other contributing factors may include the challenging installation process of many alternative tools, the significantly faster computation speed of `gmx order` compared to most alternatives, and its perceived force field independence.

Here, we introduce `gorder`, a tool that integrates and enhances the features of existing tools for computing order parameters. `gorder` calculates lipid order parameters for atomistic, united-atom, and coarse-grained systems, independent of force field. Additionally, it offers advanced features such as leaflet-specific order parameter calculations, construction of order parameter maps, or support for membranes with curved geometries. `gorder` can be easily installed via Rust's `cargo` package manager, configured using YAML-formatted files, and is—to the best of our knowledge—the fastest tool available for this purpose.

2. Software description

2.1. Theoretical background

If explicit hydrogen positions are available, S_{CH} order parameters can be calculated as:

$$S_{CH} = \frac{1}{2}\langle 3\cos^2\theta - 1\rangle, \tag{1}$$

where θ is the angle between the C–H bond vector and the bilayer normal, and the angular brackets represent molecular and temporal ensemble averages [70, 71]. The resulting order parameters are typically reported as $-S_{CH}$, a convention arising from NMR measurements and followed by `gorder` as well. Higher values of $-S_{CH}$ then correspond to more ordered membrane structures.

If hydrogens are not available, their positions need to be predicted. This prediction can be performed either explicitly, where the positions of the hydrogens are first predicted and then the S_{CH} order parameters are calculated as described in Equation 1, or implicitly, where the hydrogen predictions and the order parameter calculations are performed in a single step. Since `gorder` uses explicit hydrogen predictions, we do not describe the implicit method

here and instead refer the interested reader to [28]. `gorder` predicts hydrogen positions in the same way as the `buildH` tool [65], see the Supporting Information for details.
The calculation of S_{CC} order parameters also uses Equation 1, but in this case, θ represents the angle between the bond connecting two consecutive lipid beads and the bilayer normal [26]. S_{CC} order parameters are typically reported directly as S_{CC} without sign inversion, as they naturally follow the same trend as $-S_{CH}$.

2.2. Software architecture

Notable dependencies. The `gorder` tool is built on top of `groan_rs` (available from github.com/Ladme/groan_rs), an in-house developed Rust library for analyzing molecular dynamics simulations. Several dependencies used by the `groan_rs` library are worth noting. TPR file parsing is handled by `minitpr` (available from github.com/Ladme/minitpr), a fully standalone TPR-file parser implemented in pure Rust and developed in-house. XTC file reading is performed by `molly` (available from git.sr.ht/∼ma3ke/molly), a library also written in Rust, which is reportedly faster than the widely used `xdrfile` library. The `molly` library supports partial XTC frame reading, enabling the program to only read specific atom selections (such as the membrane without the surrounding water), which further enhances analysis speed. However, `groan_rs` still relies on `xdrfile` for parsing TRR files.

Architecture. The `gorder` tool uses a three-layered architecture with the input layer handling user input, the logic layer performing the analysis, and the presentation layer managing output of the results. The architecture of `gorder` with its high-level structures is depicted in Figure 1.
The analysis itself consists of two main stages. In the first stage, lipid molecules are identified and classified. A collection of atoms connected by bonds is considered to form a single molecule. Molecules sharing identical topologies and atoms of the same names are classified as the same molecule type. A single molecule may consist of multiple residues, while distinct molecule types can share residue names, if they differ in topology. Individual bonds are categorized into bond types, with order parameters subsequently calculated for each bond type involving atoms selected by the user.
In the second stage, the program processes the selected trajectory frames. For each frame, it iterates through identified molecule types, individual bond types within these molecule types, and specific bond instances, calculating and collecting order parameters. Additional operations may be performed at the level of individual bonds (e.g., selection of bonds in a specific part of the membrane or projecting order parameters onto two-dimensional maps),

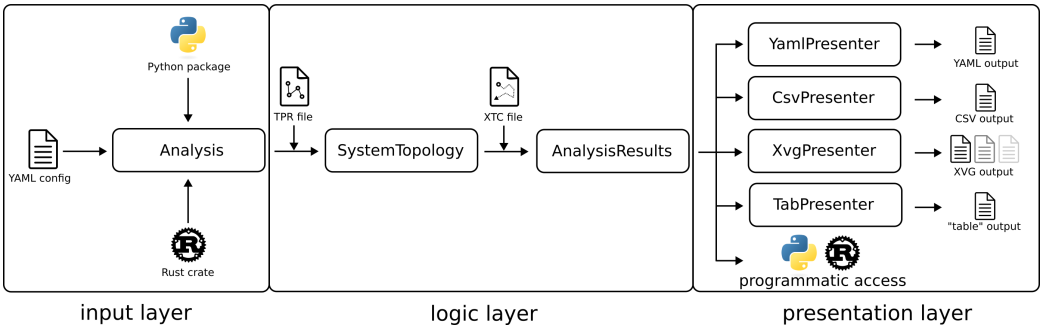

Figure 1: Simplified depiction of the architecture of `gorder`. In the input layer, the `Analysis` structure is constructed by either reading a YAML configuration file or using Python/Rust API. In the logic layer, the TPR file (or other supported topology-containing file) is read to construct a `SystemTopology` structure. Subsequently, an XTC file (or other supported trajectory file) is analyzed, generating an `AnalysisResults` structure. This structure can either be accessed programmatically via Python/Rust API or output in YAML, CSV, XVG, or a custom "table" format using presenter structures (`YamlPresenter`, `CsvPresenter`, `XvgPresenter`, `TabPresenter`).

at the level of individual molecules (e.g., leaflet classification or calculation of dynamic membrane normals), or at the level of the entire system (e.g., leaflet classification using spectral clustering).
Additional details about `gorder`'s internal implementation are provided in the Supporting Information, including descriptions of the algorithms used for membrane leaflet classification and dynamic membrane normal calculations, as well as the multithreading scheme employed by `gorder`.

2.3. Software functionalities

`gorder` is able to calculate atomistic, united-atom, and coarse-grained lipid order parameters. It is completely force field independent, which, however, requires the user to provide system connectivity and manually select atoms for the analysis. System connectivity can be supplied by providing a GROMACS TPR file, a PDB file with a connectivity section, or a custom "bonds" file. To simplify atom selection, we implemented a flexible selection language similar to that used by VMD [62], with added support for regular expressions and GROMACS NDX file groups (see the guide at ladme.github.io/gsl-guide). While `gorder` primarily expects the trajectory to be provided in the XTC file format, TRR and GRO trajectories are also supported.
The main functionalities of `gorder` include:

- Reporting order parameters for individual atom types (in atomistic and united-atom systems) as well as for individual bond types.

- Automatic classification of lipid types and their simultaneous analysis, with results reported separately for each lipid type.
- Leaflet-wise order parameter calculations, with automatic or manual assignment of lipids into leaflets.
- Estimating errors using block averaging and reporting on simulation convergence.
- Projecting lipid order parameters onto two-dimensional maps.
- Calculating order parameters for dynamically selected membrane regions.
- Dynamically computing membrane normals based on the current membrane shape, enabling reliable order parameter calculations even for curved membranes, such as vesicles, tubes, or buckled membranes.
- Automatic handling of periodic boundary conditions in orthogonal simulation boxes.
- Multithreading, with binary reproducible output independent of the number of threads used.
- Quality-of-life features, including trajectory concatenation and selection of time ranges for analysis.
- Outputting the results in YAML, CSV, or XVG formats, or in a custom "table" format designed for human readability.

All functionalities of `gorder` are configurable via a YAML-formatted configuration file. `gorder` is available as a command-line application, a Python package, and a Rust crate, facilitating seamless integration into user workflows.
For more information about the functionalities and limitations of `gorder`, we provide a comprehensive manual for the tool, accessible at ladme.github.io/gorder-manual or from doi.org/10.5281/zenodo.15282375.

3. Illustrative examples

3.1. Single-component atomistic membrane

In the first example, we calculated order parameters for both tails of POPC lipids in a planar POPC bilayer. The system contained 256 lipids represented

using the CHARMM36 force field [72] and simulated for 200 ns. The trajectory comprised 10,000 frames. The full system consisted of around 64,500 atoms. Complete simulation parameters are provided in the Supporting Information.

We focused on comparing results obtained by `gorder` with those calculated by other software and benchmarking performance, as detailed in Figure 2. Note that while we display only order parameters for carbons here, `gorder` also calculates order parameters for individual carbon-hydrogen bonds, as shown in Figure S2.

`gorder` yields results consistent with other tested tools while being significantly faster. Note that for more complex lipid compositions than presented here, `gorder` will be even more efficient since it can calculate order parameters separately for all lipid types in one trajectory pass, while all other programs require at least one pass *per* analyzed lipid type.

We also performed the same analyses and benchmarks for single-component united-atom and coarse-grained phospholipid membranes. In all cases, `gorder` matches the results of other (correctly performing) analysis tools while maintaining faster performance (see Figures S3 and S4). To further validate hydrogen position predictions in united-atom systems, we also computed united-atom order parameters for an atomistic system and compared them with atomistic order parameters (see Figure S5).

3.2. Membrane with complex composition

This example demonstrates `gorder`'s capability to analyze membranes with complex lipid compositions and estimate calculation errors. We simulated a symmetric CHARMM36 [72] membrane containing eight lipid species: POPC, POPE, POPG, POPA, DOPC, DOPE, DPPC, and PVCL2 (a cardiolipin with two palmitoyl and two oleoyl tails and a 2− charge), with 32 molecules of each type. The analysis was performed using 25,000 frames from a 500 ns trajectory segment. Complete simulation parameters are provided in the Supporting Information.

See Figure 3 for the configuration YAML file specifying analysis parameters and calculated order parameters for individual carbon atoms in each lipid tail. Note that the analysis for all lipid types is performed simultaneously at almost the same total speed as for a single-component membrane (see Figure S6).

3.3. Membrane with a phospholipid scramblase

In this example, we showcase `gorder`'s ability to create two-dimensional order parameter maps that quantify membrane order in individual regions. We also illustrate a simple, flip-flop-safe leaflet classification method. For this

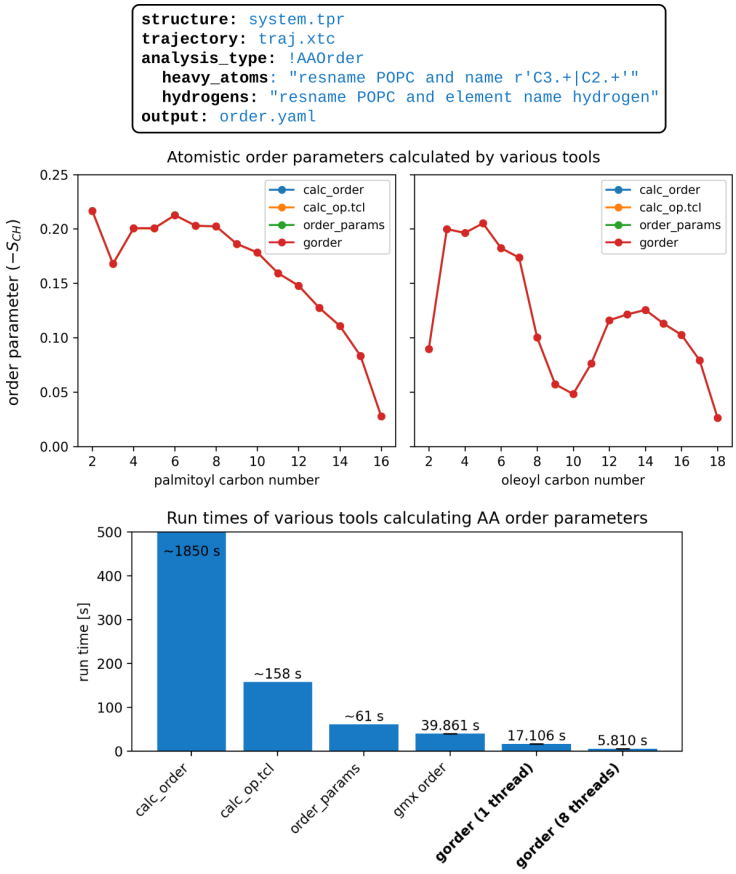

Figure 2: Calculation of order parameters in an atomistic system using `gorder` and comparison with other software. **Top:** Configuration YAML file specifying the analysis parameters for `gorder`. Structure and topology will be read from `system.tpr` and the trajectory from `traj.xtc`. Atomistic order parameters will be calculated (`!AAOrder`). The query for `heavy_atoms` selects carbons of palmitoyl and oleoyl tails, while the query for `hydrogens` selects all hydrogens of POPC molecules. The tool will automatically identify bonds between the selected atoms. Output will be written into `order.yaml` in YAML format. **Center:** Order parameters calculated by `gorder` for palmitoyl and oleoyl tails of POPC (red line), compared with results from other tools (NMR Lipids' `calc_order` script, VMD's `calc_op.tcl`, and LOOS library's `order_params`). All tools yield consistent results. **Bottom:** Execution times for order parameter calculations of POPC tail carbons across different tools. `gmx order` is included despite being designed only for fully saturated united-atom lipid tails, as it remains commonly used for atomistic systems. Benchmarking was performed on GNU/Linux Mint 20.2 (8-core Intel Core i7-11700, Samsung 870 EVO SSD) with cold cache using `hyperfine`. `gorder` was compiled using `rustc` v1.82.0 and `gcc` v9.4.0. `gorder` and `gmx order` were executed 5 times each, while the other, slower tools were run once. Note: `order_params` and `gmx order` require two runs to analyze both lipid tails. Even for a single-tail analysis (single run), `gorder` maintains significantly higher performance with comparable resources (`gorder`: 11.4 s, `gmx order`: 20.7 s).

```yaml
structure: system.tpr
trajectory: traj.xtc
analysis_type: !CGOrder
  heavy_atoms: >-
    (@membrane and name r'C3.+|C2.+') or
    (resname PVCL2 and name r'C[ABCD].+')
  hydrogens: "element name hydrogen"
estimate_error: true
output: order.yaml
```

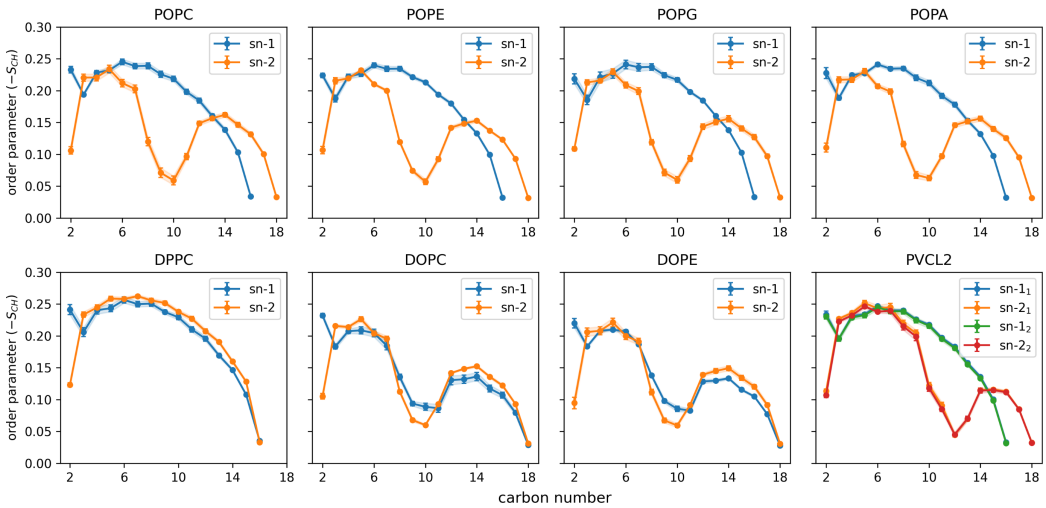

Figure 3: Calculation of order parameters in an atomistic membrane with complex lipid composition. **Top:** Configuration YAML file specifying the analysis parameters for `gorder`. The query for `heavy_atoms` selects all palmitoyl and oleoyl carbons of all lipid types. The specific lipid types are identified automatically. Error estimation is requested using `estimate_error: true`. **Bottom:** Order parameters calculated by `gorder` for carbons of individual lipid molecule types in a single analysis run. Each line corresponds to a specific lipid tail (sn-1, sn-2) of a specific lipid type. Shading represents analysis error estimated by the program using block averaging.

demonstration, we use a simulation of a Martini 3 [67] POPC membrane containing a dimer of voltage-dependent anion channel (VDAC), a common outer mitochondrial membrane protein with scramblase activity [73]. Simulation parameters are described in [73]. The analyzed trajectory segment spanned 2.5 µs (25,000 frames). Before analysis, the VDAC dimer in all trajectory frames was centered in the simulation box and RMSD-aligned to its reference structure from the first frame. Without this alignment, the projected order parameters would be spatially averaged out, obscuring the protein's effects on membrane structure.

See Figure 4 for the configuration YAML file with analysis parameters, calculated order parameters for individual bonds, and examples of xy-plane order parameter projections ("ordermaps").

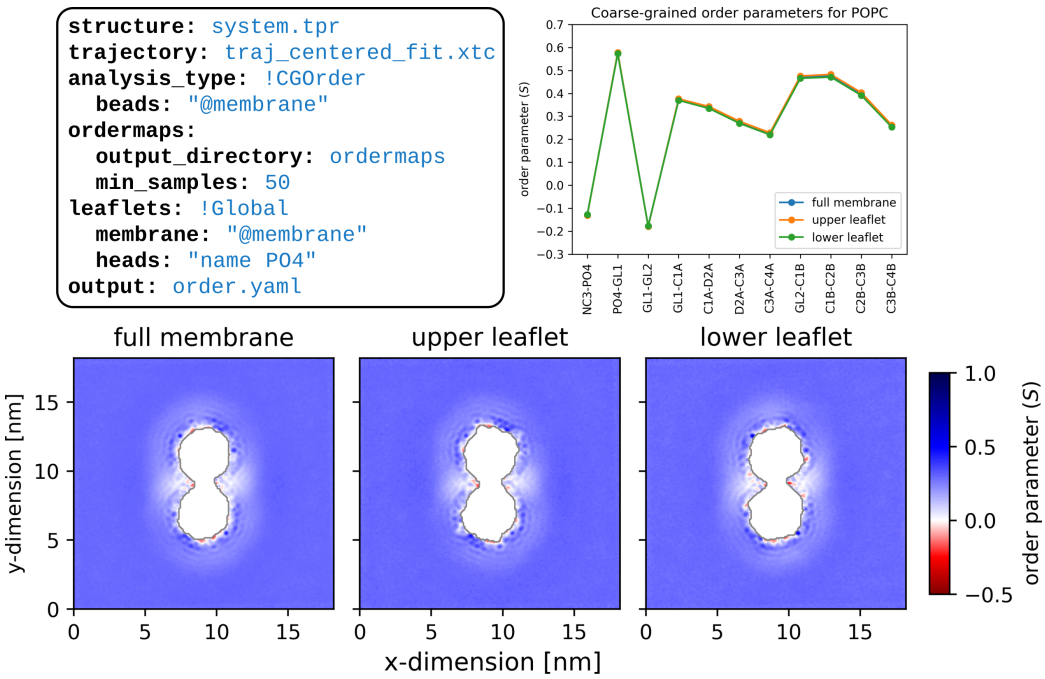

Figure 4: Calculation of order parameters in a coarse-grained membrane containing a phospholipid scramblase. **Top left**: Configuration YAML file specifying the analysis parameters for `gorder`. The analysis includes all beads of membrane lipids. Order parameter projections ("ordermaps") are written to the `ordermaps` directory. Each bin of the "ordermap" requires a minimum of 50 samples; bins with fewer samples are assigned *NaN*. The default bin size is 1×1 Å. Lipid leaflet assignment is determined in each trajectory frame by the position of the selected headgroup atom (`name PO4`, the phosphate bead) relative to the membrane's center of geometry. **Top right**: Coarse-grained order parameters for individual POPC lipid bonds in the full membrane, upper leaflet, and lower leaflet. The order parameters are nearly identical between leaflets. **Bottom**: xy-plane projections ("ordermaps") of average order parameters for all bonds of all lipid molecules in the full membrane and in each leaflet. The gray-outlined white area in each chart represents the protein dimer, where no lipids are present. Protein presence disrupts local membrane structure, visible as reduced order parameters ($S \approx 0$) or even anti-order ($S < 0$) near the protein. While only average order parameter maps are shown here, `gorder` additionally generates individual maps for each bond type and for heavy atom types in atomistic/united-atom systems.

3.4. Buckled membrane

This example demonstrates `gorder`'s ability to calculate order parameters in buckled membranes, identify leaflets in such curved systems, and compute order parameters for membrane region within a specified geometric shape. We analyzed a segment of an atomistic simulation of an artificially buckled POPC membrane (1004 lipid molecules, CHARMM36 force field [72], 400 ns duration, 10,000 frames). Prior to analysis, the membrane was aligned to fix

the positions of its curvature maximum and minimum. For full simulation parameters, see the Supporting Information.
As shown in Figure 5, the average order parameters in a buckled membrane are nearly identical to those in a flat membrane of the same composition. However, dramatic differences emerge when comparing regions with positive versus negative curvature. Specifically, lipid tails in positively curved regions exhibit significantly higher order than those in negatively curved regions. This is because positive curvature compresses lipid tails relative to their headgroups, enforcing more ordered conformations, whereas negative curvature expands the conformational space available to the tails, resulting in disordering. These results also agree with previous findings [74].
`gorder` can also calculate order parameters for membrane vesicles, as shown in Figure S7. Here, the trends are similar to the buckled membrane, with the inner (negatively curved) leaflet displaying reduced order parameters compared to the outer leaflet.

4. Impact

Lipid order parameters are commonly calculated properties of membrane systems, typically used for force field development [1, 2, 3, 4, 5, 6, 7, 67], characterization of membrane structural properties [8, 9, 10, 11, 12, 13, 14, 15], or validation of new simulation approaches [18, 19, 20, 30, 38].
With `gorder`, we bundle together the features of previously existing programs for lipid order calculations available in the GROMACS community while reimplementing them in a computationally efficient way. Our primary goal is to eliminate the problematic usage of the `gmx order` tool and the artifacts it produces. Although these artifacts may not affect the scientific validity of the results in most cases, their frequent neglect is concerning. The continued widespread use of `gmx order` indicates a clear need for a lipid order analysis tool that is more robust, while remaining at least equally simple to use and at least as computationally efficient. We believe that `gorder` fulfills these requirements completely.
Moreover, `gorder`'s features enable comprehensive exploration of membrane properties across diverse systems. By automatically identifying lipid types and calculating order parameters separately for each of them in a single pass through the trajectory, `gorder` streamlines the analysis of membranes with complex lipid compositions—systems that are increasingly common in molecular simulations. Combined with its computational efficiency, `gorder` is particularly well-suited for analyzing large, complex membranes with biologically relevant lipid compositions.

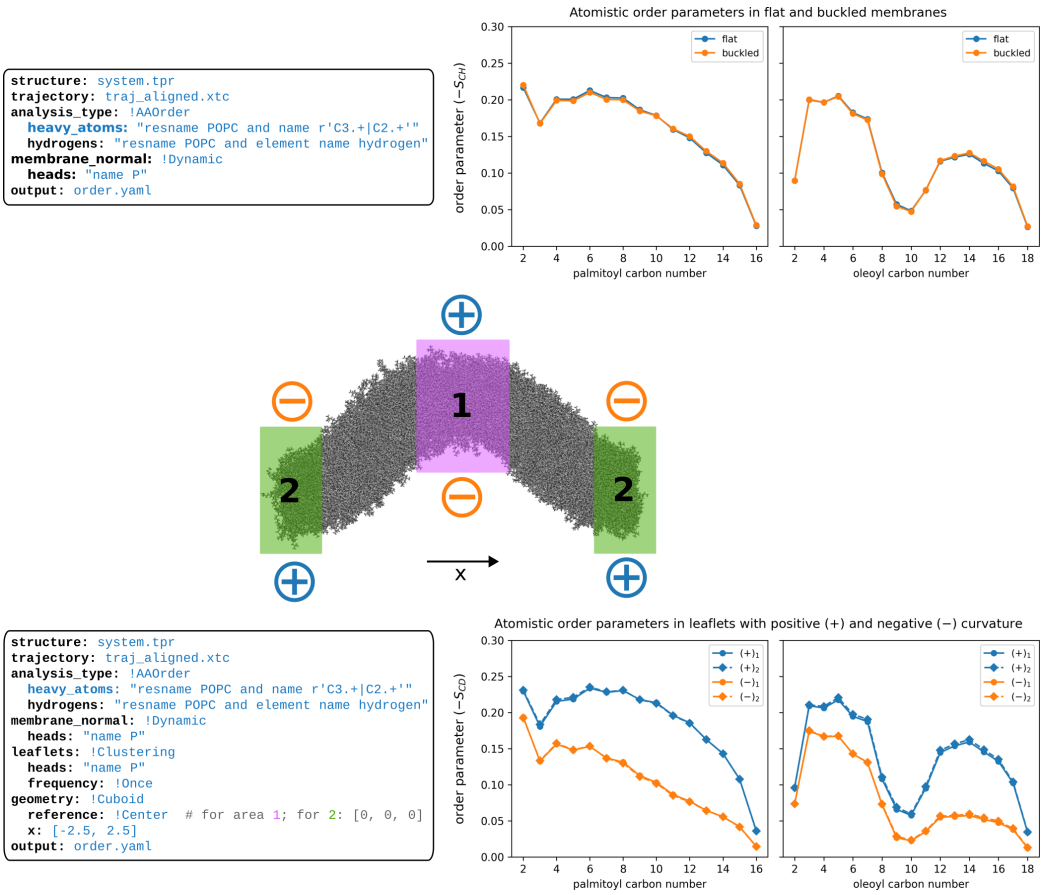

Figure 5: Calculation of order parameters in an atomistic buckled membrane. **Top left:** Configuration YAML file specifying analysis parameters, performing calculations with dynamic membrane normals (no leaflet assignment). All lipids in the membrane are analyzed, no matter their position. **Top right:** Order parameter comparison between buckled and flat POPC membranes. Average values remain nearly identical despite curvature differences. **Center:** Simulation snapshot showing the buckled membrane with labeled leaflet curvatures ((+) convex, (−) concave) and regions analyzed in the next part (purple and green rectangles). **Bottom left:** Configuration YAML file for region-specific analysis. Two analyses were performed, selecting bonds within one of two cuboidal regions. Both regions extend infinitely in the yz-plane while spanning 5 nm along the x-axis and are centered at either the simulation box center (region 1, purple) or the box origin (region 2, green). Lipid leaflet assignment uses the clustering method, performed only for the first frame (due to absent lipid flip-flop) and applied to all subsequent frames. **Bottom right:** Curvature-dependent order parameters. Identical leaflet curvatures yield matching order parameters in both regions, while opposing curvatures show significant differences, as discussed in the main text.

The ability of `gorder` to dynamically identify membrane leaflets, even in curved membranes, also simplifies the characterization of structural proper-

ties of individual leaflets, especially in membranes with lipid flip-flop. Furthermore, the tool facilitates the characterization of membrane properties near transmembrane proteins or other structures through two-dimensional order parameter projections and by enabling calculations in dynamically selected membrane regions (e.g., in the vicinity of the protein). Notably, `gorder` can calculate lipid order parameters in membranes with curved geometries, such as vesicles, buckled membranes, or tubes, enabling robust structural characterization of lipids in these complex systems.

We believe `gorder` is useful even for basic analysis tasks—arguably already relatively well-supported by other simulation programs—as it offers unprecedented speed and various quality-of-life improvements. These include automatic trajectory concatenation, seamless handling of periodic boundary conditions in orthogonal simulation boxes, and flexible selection of time range for analysis. `gorder` is independent of force field and resolution eliminating the need for multiple specialized programs for different simulation approaches.

Finally, `gorder` demonstrates that the Rust programming language can effectively support the development of complex, high-performance scientific software for analysis of molecular simulations—a domain traditionally dominated by C, C++, and Fortran.

5. Conclusions

In this work, we introduce `gorder`, a new computational tool for calculating lipid order parameters in atomistic, united-atom, and coarse-grained molecular systems, with primary support for GROMACS simulations.

The `gorder` tool is completely force field independent, has superior computational performance compared to existing alternatives, and provides extensive functionality for performing complex analyses of diverse membrane systems, including those with non-planar geometries.

`gorder` is distributed as free software under the MIT License. It is available in multiple forms: as a command-line application, a Python package, and a Rust crate. The tool can be obtained from crates.io/crates/gorder and github.com/Ladme/gorder, with comprehensive documentation available at ladme.github.io/gorder-manual. The offline version of the manual and raw results from the performed analyses are available from doi.org/10.5281/zenodo.15282375.

CRediT authorship contribution statement

Ladislav Bartoš: Conceptualization; Methodology; Investigation; Data curation; Software; Writing – original draft preparation. **Peter Pajtinka:** Methodology; Investigation; Validation; Writing – original draft preparation;

Writing – review & editing. **Robert Vácha:** Funding acquisition; Project administration; Resources; Supervision; Writing – review & editing.

Declaration of Generative AI and AI-assisted technologies in the writing process

During the preparation of this work, the authors used large language models for editorial corrections and proofreading of the manuscript. The authors reviewed and edited the generated content and take full responsibility for it.

Acknowledgements

We thank the members of the RoVa Research Group for testing and feature suggestions. The work was supported by the European Research Council (ERC) under the European Union's Horizon 2020 research and innovation programme (Grant Agreement No. 101001470) and the project National Institute of virology and bacteriology (Programme EXCELES, ID Project No. LX22NPO5103) – Funded by the European Union – Next Generation EU. Computational resources were provided by the CESNET, CERIT Scientific Cloud, and IT4 Innovations National Supercomputing Center by MEYS CR through the e-INFRA CZ (ID: 90254).

References

[1] A. P. Lyubartsev, A. L. Rabinovich, Force Field Development for Lipid Membrane Simulations, Biochimica et Biophysica Acta (BBA) - Biomembranes 1858 (10) (2016) 2483–2497. doi:10.1016/j.bbamem.2015.12.033.
URL https://linkinghub.elsevier.com/retrieve/pii/S0005273615004393

[2] R. W. Pastor, A. D. MacKerell, Development of the CHARMM Force Field for Lipids, The Journal of Physical Chemistry Letters 2 (13) (2011) 1526–1532. doi:10.1021/jz200167q.
URL https://pubs.acs.org/doi/10.1021/jz200167q

[3] Y. Yu, A. Krämer, R. M. Venable, B. R. Brooks, J. B. Klauda, R. W. Pastor, CHARMM36 Lipid Force Field with Explicit Treatment of Long-Range Dispersion: Parametrization and Validation for Phosphatidylethanolamine, Phosphatidylglycerol, and Ether Lipids, Journal of Chemical Theory and Computation 17 (3) (2021) 1581–1595. doi:10.1021/acs.jctc.0c01327.
URL https://pubs.acs.org/doi/10.1021/acs.jctc.0c01327

[4] C. J. Dickson, B. D. Madej, A. Skjevik, R. M. Betz, K. Teigen, I. R. Gould, R. C. Walker, Lipid14: The Amber Lipid Force Field, Journal of Chemical Theory and Computation 10 (2) (2014) 865–879. doi:10.1021/ct4010307.
URL https://pubs.acs.org/doi/10.1021/ct4010307

[5] C. J. Dickson, R. C. Walker, I. R. Gould, Lipid21: Complex Lipid Membrane Simulations with AMBER, Journal of Chemical Theory and Computation 18 (3) (2022) 1726–1736. doi:10.1021/acs.jctc.1c01217.
URL https://pubs.acs.org/doi/10.1021/acs.jctc.1c01217

[6] I. Ermilova, A. P. Lyubartsev, Extension of the Slipids Force Field to Polyunsaturated Lipids, The Journal of Physical Chemistry B 120 (50) (2016) 12826–12842. doi:10.1021/acs.jpcb.6b05422.
URL https://pubs.acs.org/doi/10.1021/acs.jpcb.6b05422

[7] N. Kamiya, M. Kayanuma, H. Fujitani, K. Shinoda, A New Lipid Force Field (FUJI), Journal of Chemical Theory and Computation 16 (6) (2020) 3664–3676. doi:10.1021/acs.jctc.9b01195.
URL https://pubs.acs.org/doi/10.1021/acs.jctc.9b01195

[8] S. Moradi, A. Nowroozi, M. Shahlaei, Shedding light on the structural properties of lipid bilayers using molecular dynamics simulation: a review study, RSC Advances 9 (8) (2019) 4644–4658. doi:10.1039/C8RA08441F.
URL https://xlink.rsc.org/?DOI=C8RA08441F

[9] M. Doktorova, G. Khelashvili, R. Ashkar, M. F. Brown, Molecular simulations and NMR reveal how lipid fluctuations affect membrane mechanics, Biophysical Journal 122 (6) (2023) 984–1002. doi:10.1016/j.bpj.2022.12.007.
URL https://linkinghub.elsevier.com/retrieve/pii/S0006349522038954

[10] X. Zhuang, J. R. Makover, W. Im, J. B. Klauda, A systematic molecular dynamics simulation study of temperature dependent bilayer structural properties, Biochimica et Biophysica Acta (BBA) - Biomembranes 1838 (10) (2014) 2520–2529. doi:10.1016/j.bbamem.2014.06.010.
URL https://linkinghub.elsevier.com/retrieve/pii/S0005273614002193

[11] O. S. Ollila, G. Pabst, Atomistic resolution structure and dynamics of lipid bilayers in simulations and experiments, Biochimica et Biophysica Acta (BBA) - Biomembranes 1858 (10) (2016) 2512–2528.

doi:10.1016/j.bbamem.2016.01.019.
URL https://linkinghub.elsevier.com/retrieve/pii/S0005273616300189

[12] G. A. Pantelopulos, J. E. Straub, Regimes of Complex Lipid Bilayer Phases Induced by Cholesterol Concentration in MD Simulation, Biophysical Journal 115 (11) (2018) 2167–2178. doi:10.1016/j.bpj.2018.10.011.
URL https://linkinghub.elsevier.com/retrieve/pii/S0006349518311585

[13] X. Zhuang, E. M. Dávila-Contreras, A. H. Beaven, W. Im, J. B. Klauda, An extensive simulation study of lipid bilayer properties with different head groups, acyl chain lengths, and chain saturations, Biochimica et Biophysica Acta (BBA) - Biomembranes 1858 (12) (2016) 3093–3104. doi:10.1016/j.bbamem.2016.09.016.
URL https://linkinghub.elsevier.com/retrieve/pii/S0005273616303145

[14] V. Monje-Galvan, J. B. Klauda, Modeling Yeast Organelle Membranes and How Lipid Diversity Influences Bilayer Properties, Biochemistry 54 (45) (2015) 6852–6861. doi:10.1021/acs.biochem.5b00718.
URL https://pubs.acs.org/doi/10.1021/acs.biochem.5b00718

[15] A. J. Sodt, M. L. Sandar, K. Gawrisch, R. W. Pastor, E. Lyman, The Molecular Structure of the Liquid-Ordered Phase of Lipid Bilayers, Journal of the American Chemical Society 136 (2) (2014) 725–732. doi:10.1021/ja4105667.
URL https://pubs.acs.org/doi/10.1021/ja4105667

[16] Q. Waheed, R. Tjörnhammar, O. Edholm, Phase Transitions in Coarse-Grained Lipid Bilayers Containing Cholesterol by Molecular Dynamics Simulations, Biophysical Journal 103 (10) (2012) 2125–2133. doi:10.1016/j.bpj.2012.10.014.
URL https://linkinghub.elsevier.com/retrieve/pii/S0006349512011198

[17] P. Khakbaz, J. B. Klauda, Investigation of phase transitions of saturated phosphocholine lipid bilayers via molecular dynamics simulations, Biochimica et Biophysica Acta (BBA) - Biomembranes 1860 (8) (2018) 1489–1501. doi:10.1016/j.bbamem.2018.04.014.
URL https://linkinghub.elsevier.com/retrieve/pii/S0005273618301329

[18] B. Loubet, W. Kopec, H. Khandelia, Accelerating All-Atom MD Simulations of Lipids Using a Modified Virtual-Sites Technique, Journal of Chemical Theory and Computation 10 (12) (2014) 5690–5695. doi:10.1021/ct500100f.
URL https://pubs.acs.org/doi/10.1021/ct500100f

[19] H. A. F. Santos, D. Vila-Viçosa, V. H. Teixeira, A. M. Baptista, M. Machuqueiro, Constant-pH MD Simulations of DMPA/DMPC Lipid Bilayers, Journal of Chemical Theory and Computation 11 (12) (2015) 5973–5979. doi:10.1021/acs.jctc.5b00956.
URL https://pubs.acs.org/doi/10.1021/acs.jctc.5b00956

[20] D. Hakobyan, A. Heuer, 2D lattice model of a lipid bilayer: Microscopic derivation and thermodynamic exploration, The Journal of Chemical Physics 146 (6) (2017) 064305. doi:10.1063/1.4975163.
URL https://pubs.aip.org/jcp/article/146/6/064305/316007/2D-lattice-model-of-a-lipid-bilayer-Microscopic

[21] J. Seelig, N. Waespe-Sarcevic, Molecular order in cis and trans unsaturated phospholipid bilayers, Biochemistry 17 (16) (1978) 3310–3315. doi:10.1021/bi00609a021.
URL https://pubs.acs.org/doi/abs/10.1021/bi00609a021

[22] J. Douliez, A. Léonard, E. Dufourc, Restatement of order parameters in biomembranes: calculation of C-C bond order parameters from C-D quadrupolar splittings, Biophysical Journal 68 (5) (1995) 1727–1739. doi:10.1016/S0006-3495(95)80350-4.
URL https://linkinghub.elsevier.com/retrieve/pii/S0006349595803504

[23] M. Hong, K. Schmidt-Rohr, A. Pines, NMR Measurement of Signs and Magnitudes of C-H Dipolar Couplings in Lecithin, Journal of the American Chemical Society 117 (11) (1995) 3310–3311. doi:10.1021/ja00116a051.
URL https://pubs.acs.org/doi/abs/10.1021/ja00116a051

[24] J. D. Gross, D. E. Warschawski, R. G. Griffin, Dipolar Recoupling in MAS NMR: A Probe for Segmental Order in Lipid Bilayers, Journal of the American Chemical Society 119 (4) (1997) 796–802. doi:10.1021/ja962951b.
URL https://pubs.acs.org/doi/10.1021/ja962951b

[25] D. E. Warschawski, P. F. Devaux, Order parameters of unsaturated phospholipids in membranes and the effect of cholesterol: a 1H–13C solid-state NMR study at natural abundance, European Biophysics Journal 34 (8) (2005) 987–996. doi:10.1007/s00249-005-0482-z.
URL http://link.springer.com/10.1007/s00249-005-0482-z

[26] S. Seo, M. Murata, W. Shinoda, Pivotal Role of Interdigitation in Interleaflet Interactions: Implications from Molecular Dynamics Simulations, The Journal of Physical Chemistry Letters 11 (13) (2020) 5171–5176. doi:10.1021/acs.jpclett.0c01317.
URL https://pubs.acs.org/doi/10.1021/acs.jpclett.0c01317

[27] M. J. Abraham, T. Murtola, R. Schulz, S. Páll, J. C. Smith, B. Hess, E. Lindahl, GROMACS: High performance molecular simulations through multi-level parallelism from laptops to supercomputers, SoftwareX 1-2 (2015) 19–25. doi:10.1016/j.softx.2015.06.001.
URL https://linkinghub.elsevier.com/retrieve/pii/S2352711015000059

[28] T. J. Piggot, J. R. Allison, R. B. Sessions, J. W. Essex, On the Calculation of Acyl Chain Order Parameters from Lipid Simulations, Journal of Chemical Theory and Computation 13 (11) (2017) 5683–5696. doi:10.1021/acs.jctc.7b00643.
URL https://pubs.acs.org/doi/10.1021/acs.jctc.7b00643

[29] M. Abraham, A. Alekseenko, B. Andrews, V. Basov, P. Bauer, H. Bird, E. Briand, A. Brown, M. Doijade, G. Fiorin, S. Fleischmann, S. Gorelov, G. Gouaillardet, A. Gray, M. E. Irrgang, F. Jalalypour, P. Johansson, C. Kutzner, G. Łazarski, J. A. Lemkul, M. Lundborg, P. Merz, V. Miletić, D. Morozov, L. Müllender, J. Nabet, S. Páll, A. Pasquadibisceglie, M. Pellegrino, N. Piasentin, D. Rapetti, M. U. Sadiq, H. Santuz, R. Schulz, M. Shirts, T. Shugaeva, A. Shvetsov, P. Turner, A. Villa, S. Wingbermühle, B. Hess, E. Lindahl, GROMACS 2025.1 Manual, version Number: 2025.1 (Mar. 2025). doi:10.5281/zenodo.15006631.
URL https://doi.org/10.5281/zenodo.15006631

[30] J. G. Rosas Jiménez, B. Fábián, G. Hummer, Faster Sampling in Molecular Dynamics Simulations with TIP3P-F Water, Journal of Chemical Theory and Computation 20 (24) (2024) 11068–11081. doi:10.1021/acs.jctc.4c00990.
URL https://pubs.acs.org/doi/10.1021/acs.jctc.4c00990

[31] L. Zhao, L. Liu, H. Li, L. Zhao, Z. Cao, Molecular dynamics simulations to study the role of biphenylalanine in promoting the antibacterial activity of ultrashort peptides, Journal of Molecular Graphics and Modelling 117 (2022) 108282. doi:10.1016/j.jmgm.2022.108282.
URL https://linkinghub.elsevier.com/retrieve/pii/S1093326322001619

[32] B. Dehury, S. Mishra, S. Panda, M. K. Singh, N. L. Simha, S. Pati, Structural Dynamics of Neutral Amino Acid Transporter SLC6A19 in Simple and Complex Lipid Bilayers, Journal of Cellular Biochemistry 126 (1) (2025) e30693. doi:10.1002/jcb.30693.
URL https://onlinelibrary.wiley.com/doi/10.1002/jcb.30693

[33] M. D. Smith, J. C. Smith, Effects of sodium and calcium chloride ionic stresses on model yeast membranes revealed by molecular dynamics simulation, Chemistry and Physics of Lipids 233 (2020) 104980. doi:10.1016/j.chemphyslip.2020.104980.
URL https://linkinghub.elsevier.com/retrieve/pii/S0009308420301110

[34] M. C. Oliveira, M. Yusupov, A. Bogaerts, R. M. Cordeiro, How do nitrated lipids affect the properties of phospholipid membranes?, Archives of Biochemistry and Biophysics 695 (2020) 108548. doi:10.1016/j.abb.2020.108548.
URL https://linkinghub.elsevier.com/retrieve/pii/S0003986120305579

[35] S. Mishra, M. Rout, M. K. Singh, B. Dehury, S. Pati, Illuminating the structural basis of human neurokinin 1 receptor (NK1R) antagonism through classical all-atoms molecular dynamics simulations, Journal of Cellular Biochemistry 124 (11) (2023) 1848–1869. doi:10.1002/jcb.30493.
URL https://onlinelibrary.wiley.com/doi/10.1002/jcb.30493

[36] B. Dehury, N. Tang, R. Mehra, T. L. Blundell, K. P. Kepp, Side-by-side comparison of Notch- and C83 binding to -secretase in a complete membrane model at physiological temperature, RSC Advances 10 (52) (2020) 31215–31232. doi:10.1039/D0RA04683C.
URL https://xlink.rsc.org/?DOI=D0RA04683C

[37] D. R. Mahato, M. Andersson, Dynamic lipid interactions in the plasma membrane Na+,K+-ATPase, Biochimica et Biophysica Acta (BBA) - Molecular Cell Research 1870 (7) (2023) 119545.

doi:10.1016/j.bbamcr.2023.119545.
URL https://linkinghub.elsevier.com/retrieve/pii/S0167488923001179

[38] M. K. Hazrati, L. Sukeník, R. Vácha, Split Membrane: A New Model to Accelerate All-Atom MD Simulation of Phospholipid Bilayers, Journal of Chemical Information and Modeling 65 (2) (2025) 845–856. doi:10.1021/acs.jcim.4c01664.
URL https://pubs.acs.org/doi/10.1021/acs.jcim.4c01664

[39] D. Schoeman, R. Cloete, B. C. Fielding, The Flexible, Extended Coil of the PDZ-Binding Motif of the Three Deadly Human Coronavirus E Proteins Plays a Role in Pathogenicity, Viruses 14 (8) (2022) 1707. doi:10.3390/v14081707.
URL https://www.mdpi.com/1999-4915/14/8/1707

[40] Q. Zhang, T. Sun, F. Yu, W. Liu, J. Gao, J. Chen, H. Zheng, J. Liu, C. Miao, H. Guo, W. Tian, M. Su, Y. Guo, X. Liu, Y. Pei, Z. Wang, S. Chen, C. Mu, S. M. Lam, G. Shui, Z. Li, Z. Yu, Y. Zhang, G. Chen, C. Lu, A. C. Midgley, C. Li, X. Bian, X. Liao, Y. Wang, W. Xiong, H. Zhu, Y. Li, Q. Chen, PAFAH2 suppresses synchronized ferroptosis to ameliorate acute kidney injury, Nature Chemical Biology 20 (7) (2024) 835–846. doi:10.1038/s41589-023-01528-7.
URL https://www.nature.com/articles/s41589-023-01528-7

[41] L. Liu, L. Zhao, L. Liu, S. Yue, J. Wang, Z. Cao, Influence of Different Aromatic Hydrophobic Residues on the Antimicrobial Activity and Membrane Selectivity of BRBR-NH_2 Tetrapeptide, Langmuir 36 (50) (2020) 15331–15342. doi:10.1021/acs.langmuir.0c02777.
URL https://pubs.acs.org/doi/10.1021/acs.langmuir.0c02777

[42] W. Rangubpit, S. Sungted, J. Wong-Ekkabut, H. E. Distaffen, B. L. Nilsson, C. L. Dias, Pore Formation by Amyloid-like Peptides: Effects of the Nonpolar–Polar Sequence Pattern, ACS Chemical Neuroscience 15 (18) (2024) 3354–3362. doi:10.1021/acschemneuro.4c00333.
URL https://pubs.acs.org/doi/10.1021/acschemneuro.4c00333

[43] M. Maleš, L. Zoranić, Simulation Study of the Effect of Antimicrobial Peptide Associations on the Mechanism of Action with Bacterial and Eukaryotic Membranes, Membranes 12 (9) (2022) 891. doi:10.3390/membranes12090891.
URL https://www.mdpi.com/2077-0375/12/9/891

[44] P. L. Hernández-Adame, B. Bertrand, M. I. Escamilla-Ruiz, J. Ruiz-García, C. Munoz-Garay, Molecular and energetic analysis of the interaction and specificity of Maximin 3 with lipid membranes: In vitro and in silico assessments, Protein Science 33 (11) (2024) e5188. doi:10.1002/pro.5188.
URL https://onlinelibrary.wiley.com/doi/10.1002/pro.5188

[45] M. A. Rodriguez, I. Felsztyna, D. A. García, M. E. Sánchez-Borzone, V. Miguel, Interaction of fluralaner with binary model membranes. Potential implications in the selectivity for invertebrates/vertebrates, Journal of Molecular Liquids 403 (2024) 124891. doi:https://doi.org/10.1016/j.molliq.2024.124891.
URL https://www.sciencedirect.com/science/article/pii/S0167732224009474

[46] J. Yuan, F. Meng, Effects of cholesterol on chlorzoxazone translocation across POPC bilayer, Journal of Molecular Modeling 27 (5) (2021) 146. doi:10.1007/s00894-021-04777-2.
URL https://link.springer.com/10.1007/s00894-021-04777-2

[47] S. Kumar, R. Rana, D. K. Yadav, Atomic-scale modeling of the effect of lipid peroxidation on the permeability of reactive species, Journal of Biomolecular Structure and Dynamics 39 (4) (2021) 1284–1294. doi:10.1080/07391102.2020.1730971.
URL https://www.tandfonline.com/doi/full/10.1080/07391102.2020.1730971

[48] R.-z. Nie, M.-z. Dang, Z.-z. Ge, Y.-q. Huo, B. Yu, S.-w. Tang, Influence of the gallate moiety on the interactions between green tea polyphenols and lipid membranes elucidated by molecular dynamics simulations, Biophysical Chemistry 274 (2021) 106592. doi:10.1016/j.bpc.2021.106592.
URL https://linkinghub.elsevier.com/retrieve/pii/S0301462221000740

[49] H. Junqueira, A. P. Schroder, F. Thalmann, A. Klymchenko, Y. Mély, M. S. Baptista, C. M. Marques, Molecular organization in hydroperoxidized POPC bilayers, Biochimica et Biophysica Acta (BBA) - Biomembranes 1863 (10) (2021) 183659. doi:10.1016/j.bbamem.2021.183659.
URL https://linkinghub.elsevier.com/retrieve/pii/S0005273621001097

[50] M. Yekefallah, C. A. Rasberry, E. J. Van Aalst, H. P. Browning, R. Amani, D. B. Versteeg, B. J. Wylie, Mutational Insight into Allosteric Regulation of Kir Channel Activity, ACS Omega 7 (48) (2022) 43621–43634. doi:10.1021/acsomega.2c04456.
URL https://pubs.acs.org/doi/10.1021/acsomega.2c04456

[51] M. W. Chemao-Elfihri, M. Hakmi, H. Abbou, S. Kartti, E. E. Fahime, L. Belyamani, S. Boutayeb, Staphylococcus hominis as a source of antimicrobial peptides: identification of a new peptide with potential antimicrobial properties using in silico approach, Archives of Microbiology 207 (5) (2025) 119. doi:10.1007/s00203-025-04323-1.
URL https://link.springer.com/10.1007/s00203-025-04323-1

[52] O. Engberg, A. V. Mathath, V. Döbel, C. Frie, M. K. Lemberg, D. Chakraborty, D. Huster, Evaluating the impact of the membrane thickness on the function of the intramembrane protease GlpG, Biophysical Journal 123 (23) (2024) 4067–4081. doi:10.1016/j.bpj.2024.10.019.
URL https://linkinghub.elsevier.com/retrieve/pii/S0006349524007070

[53] L. Ou, V. Corradi, D. P. Tieleman, Q. Liang, Atomistic Simulations on Interactions between Amphiphilic Janus Nanoparticles and Lipid Bilayers: Effects of Lipid Ordering and Leaflet Asymmetry, The Journal of Physical Chemistry B 124 (22) (2020) 4466–4475. doi:10.1021/acs.jpcb.9b11989.
URL https://pubs.acs.org/doi/10.1021/acs.jpcb.9b11989

[54] A. Żak, K. Korshunova, N. Rajtar, W. Kulig, M. Kepczynski, Deciphering Lipid Arrangement in Phosphatidylserine/Phosphatidylcholine Mixed Membranes: Simulations and Experiments, Langmuir 39 (51) (2023) 18995–19007. doi:10.1021/acs.langmuir.3c03061.
URL https://pubs.acs.org/doi/10.1021/acs.langmuir.3c03061

[55] H. Korolainen, A. Olżyńska, W. Pajerski, P. Chytrosz-Wrobel, I. Vattulainen, W. Kulig, L. Cwiklik, Assessing vitamin E acetate as a proxy for E-cigarette additives in a realistic pulmonary surfactant model, Scientific Reports 14 (1) (2024) 23805. doi:10.1038/s41598-024-75301-8.
URL https://www.nature.com/articles/s41598-024-75301-8

[56] C. A. Sallaberry, B. J. Voss, W. B. Stone, F. Estrada, A. Bhatia, J. D. Soto, C. W. Griffin, C. M. Vander Zanden, Curcumin Reduces Amyloid Beta Oligomer Interactions with Anionic Membranes, ACS Chemical Neuroscience 14 (22) (2023) 4026–4038. doi:10.1021/acschemneuro.

3c00512.
URL https://pubs.acs.org/doi/10.1021/acschemneuro.3c00512

[57] D. Biriukov, M. Javanainen, Efficient Simulations of Solvent Asymmetry Across Lipid Membranes Using Flat-Bottom Restraints, Journal of Chemical Theory and Computation 19 (18) (2023) 6332–6341. doi:10.1021/acs.jctc.3c00614.
URL https://pubs.acs.org/doi/10.1021/acs.jctc.3c00614

[58] J. Eid, A. Jraij, H. Greige-Gerges, L. Monticelli, Effect of quercetin on lipid membrane rigidity: assessment by atomic force microscopy and molecular dynamics simulations, BBA Advances 1 (2021) 100018. doi:10.1016/j.bbadva.2021.100018.
URL https://linkinghub.elsevier.com/retrieve/pii/S266716032100017X

[59] R.-C. Bider, T. Lluka, S. Himbert, A. Khondker, S. M. Qadri, W. P. Sheffield, M. C. Rheinstädter, Stabilization of Lipid Membranes through Partitioning of the Blood Bag Plasticizer Di-2-ethylhexyl phthalate (DEHP), Langmuir 36 (40) (2020) 11899–11907. doi:10.1021/acs.langmuir.0c01964.
URL https://pubs.acs.org/doi/10.1021/acs.langmuir.0c01964

[60] R. Kneiszl, S. Hossain, P. Larsson, In Silico-Based Experiments on Mechanistic Interactions between Several Intestinal Permeation Enhancers with a Lipid Bilayer Model, Molecular Pharmaceutics 19 (1) (2022) 124–137. doi:10.1021/acs.molpharmaceut.1c00689.
URL https://pubs.acs.org/doi/10.1021/acs.molpharmaceut.1c00689

[61] A. M. Kiirikki, H. S. Antila, L. S. Bort, P. Buslaev, F. Favela-Rosales, T. M. Ferreira, P. F. J. Fuchs, R. Garcia-Fandino, I. Gushchin, B. Kav, N. Kučerka, P. Kula, M. Kurki, A. Kuzmin, A. Lalitha, F. Lolicato, J. J. Madsen, M. S. Miettinen, C. Mingham, L. Monticelli, R. Nencini, A. M. Nesterenko, T. J. Piggot, Piñeiro, N. Reuter, S. Samantray, F. Suárez-Lestón, R. Talandashti, O. H. S. Ollila, Overlay databank unlocks data-driven analyses of biomolecules for all, Nature Communications 15 (1) (2024) 1136. doi:10.1038/s41467-024-45189-z.
URL https://www.nature.com/articles/s41467-024-45189-z

[62] W. Humphrey, A. Dalke, K. Schulten, VMD: Visual molecular dynamics, Journal of Molecular Graphics 14 (1) (1996) 33–38. doi:10.1016/0263-7855(96)00018-5.

URL https://linkinghub.elsevier.com/retrieve/pii/0263785596000185

[63] T. Romo, A. Grossfield, LOOS: An extensible platform for the structural analysis of simulations, in: 2009 Annual International Conference of the IEEE Engineering in Medicine and Biology Society, IEEE, Minneapolis, MN, 2009, pp. 2332–2335. doi:10.1109/IEMBS.2009.5335065.
URL http://ieeexplore.ieee.org/document/5335065/

[64] T. D. Romo, N. Leioatts, A. Grossfield, Lightweight object oriented structure analysis: Tools for building tools to analyze molecular dynamics simulations, Journal of Computational Chemistry 35 (32) (2014) 2305–2318. doi:10.1002/jcc.23753.
URL https://onlinelibrary.wiley.com/doi/10.1002/jcc.23753

[65] H. Santuz, A. Bacle, P. Poulain, P. Fuchs, buildH: Build hydrogen atoms from united-atom molecular dynamics of lipids and calculate the order parameters, Journal of Open Source Software 6 (65) (2021) 3521. doi:10.21105/joss.03521.
URL https://joss.theoj.org/papers/10.21105/joss.03521

[66] S. J. Marrink, H. J. Risselada, S. Yefimov, D. P. Tieleman, A. H. De Vries, The MARTINI Force Field: Coarse Grained Model for Biomolecular Simulations, The Journal of Physical Chemistry B 111 (27) (2007) 7812–7824. doi:10.1021/jp071097f.
URL https://pubs.acs.org/doi/10.1021/jp071097f

[67] P. C. T. Souza, R. Alessandri, J. Barnoud, S. Thallmair, I. Faustino, F. Grünewald, I. Patmanidis, H. Abdizadeh, B. M. H. Bruininks, T. A. Wassenaar, P. C. Kroon, J. Melcr, V. Nieto, V. Corradi, H. M. Khan, J. Domański, M. Javanainen, H. Martinez-Seara, N. Reuter, R. B. Best, I. Vattulainen, L. Monticelli, X. Periole, D. P. Tieleman, A. H. De Vries, S. J. Marrink, Martini 3: a general purpose force field for coarse-grained molecular dynamics, Nature Methods 18 (4) (2021) 382–388. doi:10.1038/s41592-021-01098-3.
URL https://www.nature.com/articles/s41592-021-01098-3

[68] P. Smith, C. D. Lorenz, LiPyphilic: A Python Toolkit for the Analysis of Lipid Membrane Simulations, Journal of Chemical Theory and Computation 17 (9) (2021) 5907–5919. doi:10.1021/acs.jctc.1c00447.
URL https://pubs.acs.org/doi/10.1021/acs.jctc.1c00447

[69] L. Bartoš, Order - Code for Coarse-Grained Lipid Order Calculations (Sep. 2023). doi:10.5281/zenodo.8369479.
URL https://doi.org/10.5281/zenodo.8369479

[70] J. Seelig, Deuterium magnetic resonance: theory and application to lipid membranes, Quarterly Reviews of Biophysics 10 (3) (1977) 353–418. doi:10.1017/S0033583500002948.
URL https://www.cambridge.org/core/product/identifier/S0033583500002948/type/journal_article

[71] L. S. Vermeer, B. L. De Groot, V. Réat, A. Milon, J. Czaplicki, Acyl chain order parameter profiles in phospholipid bilayers: computation from molecular dynamics simulations and comparison with 2H NMR experiments, European Biophysics Journal 36 (8) (2007) 919–931. doi:10.1007/s00249-007-0192-9.
URL http://link.springer.com/10.1007/s00249-007-0192-9

[72] J. B. Klauda, R. M. Venable, J. A. Freites, J. W. O'Connor, D. J. Tobias, C. Mondragon-Ramirez, I. Vorobyov, A. D. MacKerell, R. W. Pastor, Update of the CHARMM All-Atom Additive Force Field for Lipids: Validation on Six Lipid Types, The Journal of Physical Chemistry B 114 (23) (2010) 7830–7843. doi:10.1021/jp101759q.
URL https://pubs.acs.org/doi/10.1021/jp101759q

[73] H. Jahn, L. Bartoš, G. I. Dearden, J. S. Dittman, J. C. M. Holthuis, R. Vácha, A. K. Menon, Phospholipids are imported into mitochondria by VDAC, a dimeric beta barrel scramblase, Nature Communications 14 (1) (2023) 8115. doi:10.1038/s41467-023-43570-y.
URL https://www.nature.com/articles/s41467-023-43570-y

[74] S. O. Yesylevskyy, T. Rivel, C. Ramseyer, The influence of curvature on the properties of the plasma membrane. Insights from atomistic molecular dynamics simulations, Scientific Reports 7 (1) (2017) 16078. doi:10.1038/s41598-017-16450-x.
URL https://www.nature.com/articles/s41598-017-16450-x